Title

A modular approach to creating large engineered cartilage surfaces

Authors

Ford, Audrey C

Chui, Wan Fung

Zeng, Anne Y

et al.

Publication Date

2018

DOI

10.1016/j.jbiomech.2017.11.035

Peer reviewed

Journal of Biomechanics 67 (2018) 177–183

Contents lists available at ScienceDirect

Journal of Biomechanics

journal homepage: www.elsevier.com/locate/jbiomech
www.JBiomech.com

Short communication

A modular approach to creating large engineered cartilage surfaces

Audrey C. Ford [a], Wan Fung Chui [a], Anne Y. Zeng [a], Aditya Nandy [a], Ellen Liebenberg [b], Carlo Carraro [c], Galateia Kazakia [d], Tamara Alliston [b], Grace D. O'Connell [a,*]

[a] Department of Mechanical Engineering, University of California, Berkeley, United States
[b] Department of Orthopaedic Surgery, University of California, San Francisco, United States
[c] Department of Chemical Engineering, University of California, Berkeley, United States
[d] Department of Radiology, University of California, San Francisco, United States

ARTICLE INFO

Article history:
Accepted 28 November 2017

Keywords:
Articular cartilage
Tissue engineering
Modular fabrication

ABSTRACT

Native articular cartilage has limited capacity to repair itself from focal defects or osteoarthritis. Tissue engineering has provided a promising biological treatment strategy that is currently being evaluated in clinical trials. However, current approaches in translating these techniques to developing large engineered tissues remains a significant challenge. In this study, we present a method for developing large-scale engineered cartilage surfaces through modular fabrication. Modular Engineered Tissue Surfaces (METS) uses the well-known, but largely under-utilized self-adhesion properties of *de novo* tissue to create large scaffolds with nutrient channels. Compressive mechanical properties were evaluated throughout METS specimens, and the tensile mechanical strength of the bonds between attached constructs was evaluated over time. Raman spectroscopy, biochemical assays, and histology were performed to investigate matrix distribution. Results showed that by Day 14, stable connections had formed between the constructs in the METS samples. By Day 21, bonds were robust enough to form a rigid sheet and continued to increase in size and strength over time. Compressive mechanical properties and glycosaminoglycan (GAG) content of METS and individual constructs increased significantly over time. The METS technique builds on established tissue engineering accomplishments of developing constructs with GAG composition and compressive properties approaching native cartilage. This study demonstrated that modular fabrication is a viable technique for creating large-scale engineered cartilage, which can be broadly applied to many tissue engineering applications and construct geometries.

1. Introduction

Tissue engineering has provided promising treatments for damaged or degenerated tissues. Tissue engineering utilizes a combination of biomaterials, cells, and inductive factors to promote *de novo* tissue growth both in the laboratory and *in vivo* with favorable results towards achieving native mechanical and biochemical properties (Mauck et al., 2000; DuRaine et al., 2015; Gadjanski and Vunjak-Novakovic, 2015; Makris et al., 2015; Benya and Shaffer, 1982; Awada et al., 2004; Natoli et al., 2009; Bian et al. 2010; Erickson et al., 2012; Nims et al., 2017). However, translating these techniques to larger engineered tissues (>4 mm diameter) has not been trivial (Bian et al., 2009; O'Connell et al., 2013; Cigan et al., 2014). Larger scaffolds (~10 mm diameter) have limited tissue growth and inhomogeneous matrix deposition due to limited nutrient diffusion into the center of the scaffold. Limited nutrient diffusion results in greater matrix deposition and stiffness at the periphery of the construct, which is problematic for clinical application (Farrell et al., 2012; Khoshgoftar et al., 2013; Nims et al., 2014; Kelly et al., 2006; Bian et al., 2009; Buckley et al., 2012; Nims et al., 2015).

Previously used methods for increasing nutrient diffusion in larger engineered cartilage, include macrochannels, microchannels, dynamic loading, and perfusion (Chahine et al., 2009, Eniwumide et al., 2009, Lima et al., 2012; Kock et al., 2014). Macrochannels (e.g. 1 mm diameter channel) in the center of a larger (10 mm diameter) construct increases nutrient availability throughout the construct, resulting in homogenous distribution of matrix deposition (Bian et al., 2009). Cigan et al. (2014, 2016), Nims et al. (2017). An alternative approach for increasing nutrient diffusion in larger monolithic engineered cartilage with macrochannels is to use a modular fabrication approach, which results in channels

* Corresponding author at: University of California, Berkeley, Department of Mechanical Engineering, 5122 Etcheverry Hall, #1740, Berkeley, CA 94720, United States.
E-mail address: g.oconnell@berkeley.edu (G.D. O'Connell).

https://doi.org/10.1016/j.jbiomech.2017.11.035
0021-9290/

forming between junctions of smaller constructs initially cultured individually to maximize nutrient availability.

Modular tissue engineering is a technique of initially culturing smaller components, which are combined at a later time point to create larger surfaces (Nichol and Khademhosseini, 2009). This approach has been used to combine cultured rings into tube-like constructs for tracheal reconstruction and to combine pellet cultures into larger sheets of engineered cartilage (Bhumiratana et al., 2014; Mori et al., 2014; Dikina et al., 2015; Nover et al., 2016). These platforms take advantage of the inherent adhesivity of *de novo* extracellular matrix. In this study, we describe a method to fabricate Modular Engineered Tissues Surfaces (METS) by applying the inherent adhesivity of *de novo* cartilage to a well-established cell-based agarose model for cultivating engineered cartilage (Fig. 1). The techniques applied here are broadly adaptable to other tissues or organs.

2. Methods

Chondrocytes were harvested from juvenile bovine knees (age: 3–6 weeks, n = 2–3 animals per study), digested, expanded, and encapsulated in agarose with a cell density of 30×10^6 cells/mL as previously described (O'Connell et al., 2015). Constructs were cored with dimensions of 4 mm diameter and 2.34 mm thickness and cultured in chemically-defined media (1–3 mL of media per construct; hgDMEM with 0.1 μM dexamethasone, 40 mg/mL L-proline, 50 mg/mL ascorbate 2-phosphate, 100 mg/mL sodium pyruvate, 1 × ITS+ premix, 100 U/mL penicillin, and 100 mg/mL streptomycin and amphotericin B) for 35 days and supplemented with 10 ng/mL TGF-β3 for the first 14 days (O'Connell et al., 2014).

Four studies with individual controls were conducted to evaluate the scalability of the METS design (4 mm diameter; Table 1). In the first week of culture, individual constructs were placed in 3D printed baskets to form METS (Acrylonitrile butadiene styrene, printer resolution = 0.5 mm, Dimension 1200es, Stratasys, Eden Prairie, MN; Fig. 1). 2 × 2, 3 × 3, or 5 × 5 METS were created by placing 4, 9, or 25 constructs, respectively, into 3D printed baskets (coverage area: $2 \times 2 \approx 64$ mm^2, $3 \times 3 \approx 144$ mm^2, $5 \times 5 \approx 400$ m m^2; Fig. 1C–E).

Additionally, a METS sample with patient-specific geometry was prepared by combining 75 individual constructs. A high-resolution computed tomography image of a cadaveric human tibial plateau was reconstructed into a 3D solid model using cubic spline interpolation between 2D image slices (SimVascular; Fig. 2A and B) (Cohen et al., 1999; Wilson et al., 2001). The resulting model was used to print a porous-walled culture basket, and individual constructs were cultured in the mold for two weeks (Fig. 2C and D).

Compressive mechanical properties (i.e. equilibrium and dynamic moduli) were determined in the METS at Day 0 and then weekly or biweekly to characterize matrix production (n = 4–5 per

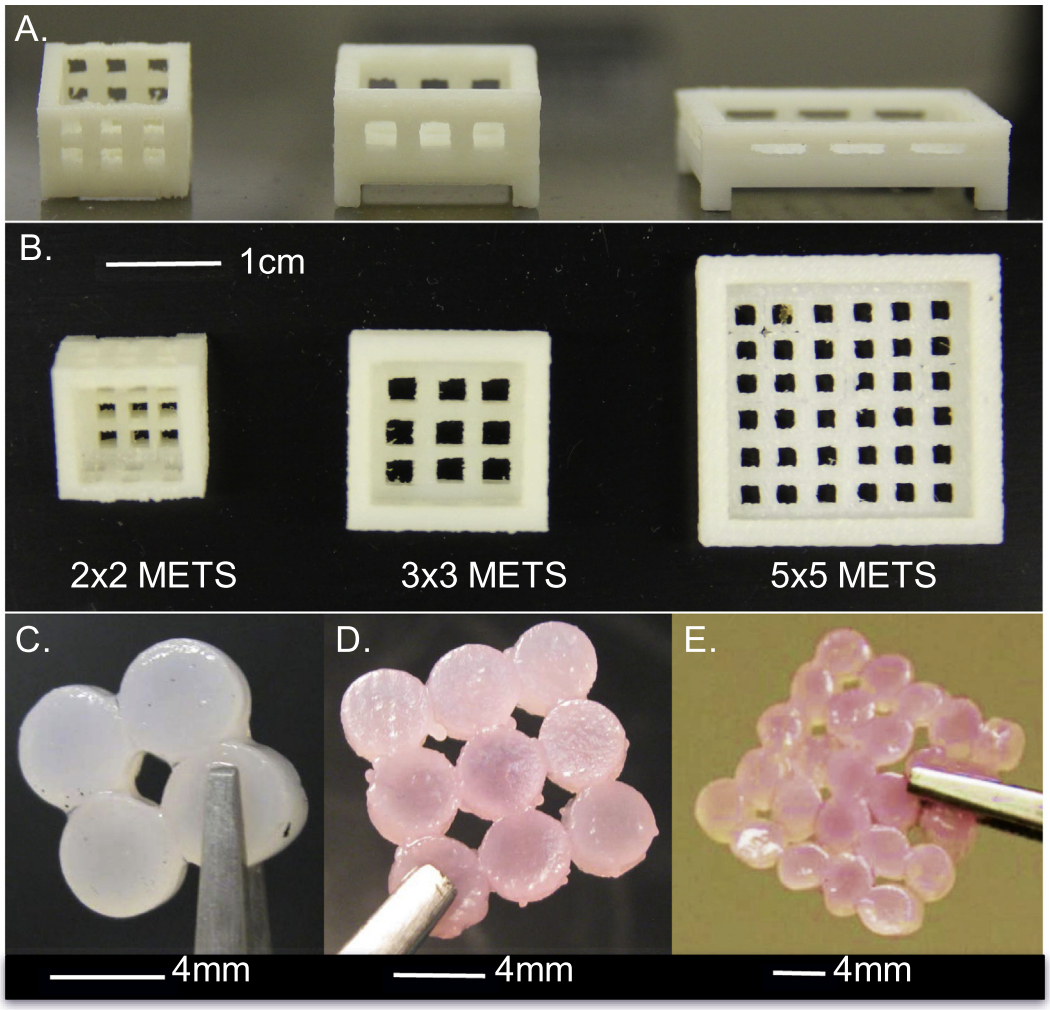

Fig. 1. (A) Side view and (B) top view of 3D printed baskets with spaces for nutrient diffusion. The top surface was open for free diffusion of culture media. Representative images from (C) 2 × 2 METS, (D) 3 × 3 METS, and (E) 5 × 5 METS.

Table 1
Outline of four studies performed to demonstrate the viability of the METS technique and evaluate location dependence of mechanical and biochemical properties in the constructs within the METS samples.

Study	Control	METS	Size (mm^2)
1			64
2			144
3			400
4	N/A	Patient specific	>950

group per time point). Equilibrium modulus was measured using an Instron 5943 in unconfined compression at 10% strain followed by a sinusoidal ±1% strain at 0.5 Hz to measure dynamic modulus. Individual constructs within METS samples were separated after culture to measure local properties.

Tensile strength of the bond was evaluated in 2×2 and 5×5 METS by pulling two constructs until bond failure (Instron 5943). In the 2×2 METS, the bond tensile strength was assessed (1 mm/min) at Days 21 and 28. In 5×5 METS, bond failure was not achievable with a strain rate of 1 mm/min due to slippage between the grips and the constructs; therefore, 1 mm/s was used (Days 14 and 28). The peak force at failure was recorded. Bond width was measured optically. Bond thickness was could not be accurately assessed; therefore, stress was not calculated.

After mechanical testing, samples were weighed, lyophilized, and reweighed. On Day 28, samples (n = 4–5 per group) were digested overnight with proteinase K (Sigma-Aldrich, St. Louis, MO). DNA, Glycosaminoglycan (GAG), and collagen content was measured using a PicoGreen (Invitrogen, Co.), a 1,9-dimethylmethylene blue (DMMB) and a hydroxyproline assay respectively.

A 3×3 METS sample was prepared for histology (Day 21). Histological slices were stained with hematoxylin and eosin to characterize cellular distribution. The patient specific METS was also prepared for raman spectroscopy and histology, stained for cellular distribution and aggrecan. Raman spectroscopy was used

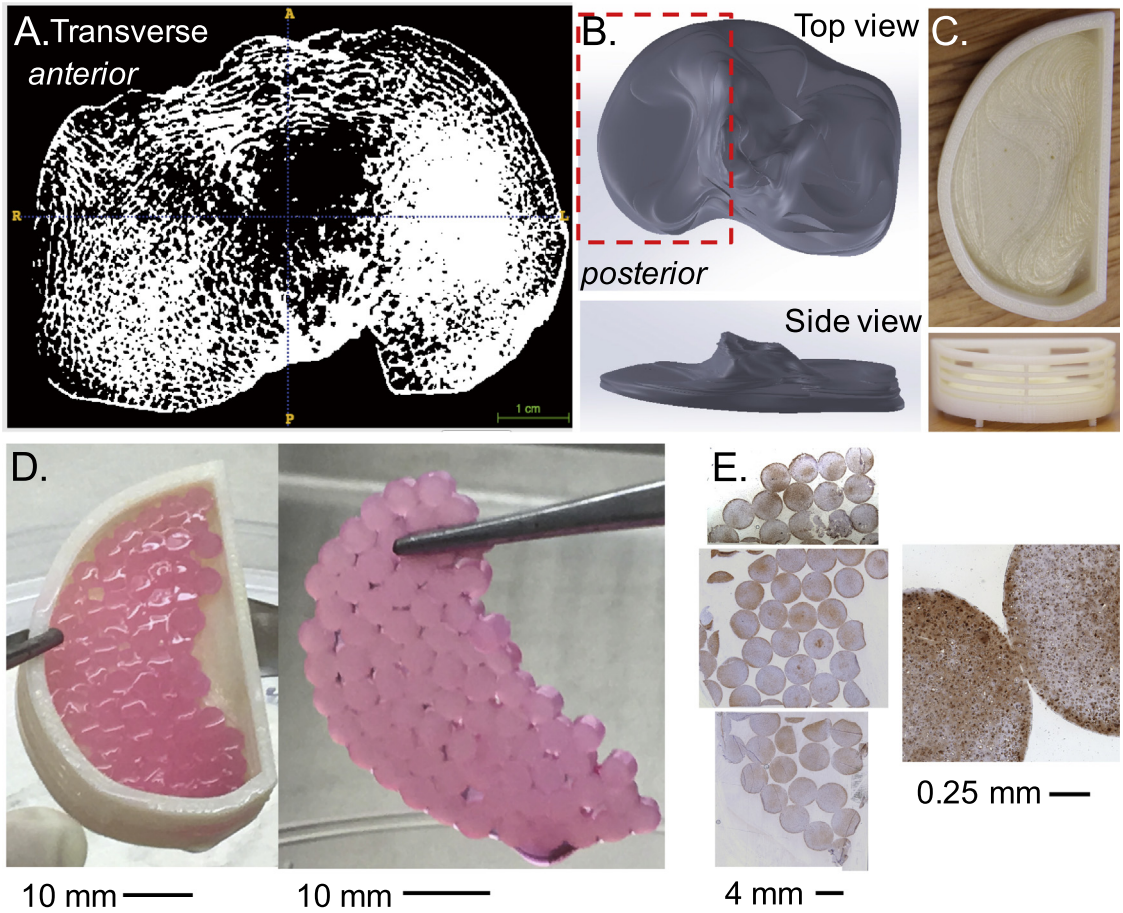

Fig. 2. (A) Transverse slice from high-resolution micro-computed tomography (μCT) of a human cadaveric tibia plateau. (B) SimVascular was used to manually outline the area in each slice and reconstructed to create a steriolithography file (STL), which was imported into SolidWorks as a 3D part. (C) The part was modified to include porous walls and created using a 3D printer. (D) Patient specific METS was created by combining 75 constructs (contact area ~950 mm^2). (E) Histological staining was positive for aggrecan throughout the construct (brown stain) with cells distributed evenly throughout (blue strain represents cell nuclei). (For interpretation of the references to colour in this figure legend, the reader is referred to the web version of this article.)

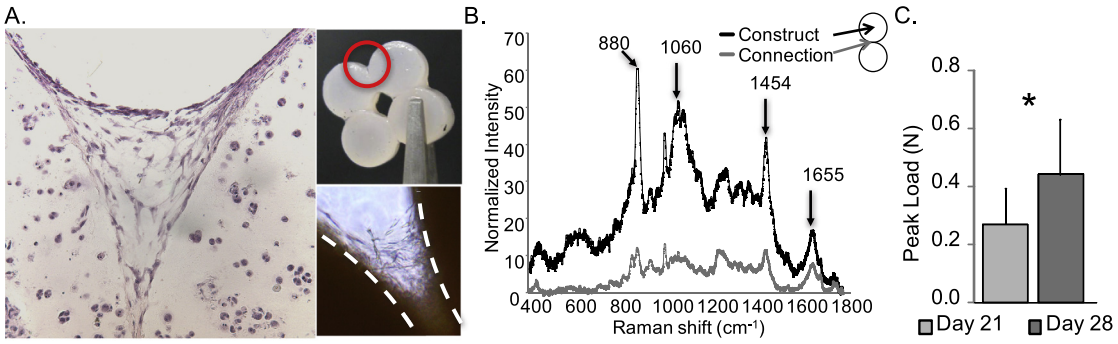

Fig. 3. (A) Hematoxylin and eosin staining showing tissue formation with cell infiltration at a bond site within a METS sample. *Inset:* (top) Representative 2 × 2 METS sample identifying region of interest and (bottom) bright-field image of fibers observed at the bond site. (B) Raman spectra comparing the METS bond and bulk construct. Peaks are attributed to the following compounds: collagen – 880 cm^{-1}, GAG – 1060 cm^{-1}, organic content – 1454 cm^{-1}, collagen – 1655 cm^{-1} (Esmonde-White, 2014). (C) Peak load at failure of METS bond increased over time (* represents $p < .05$). Data shown from 2 × 2 METS.

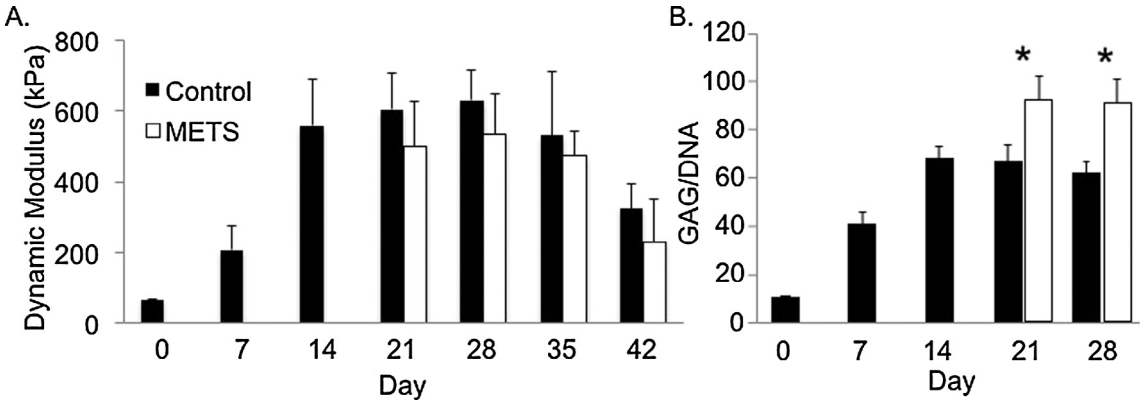

Fig. 4. (A) Compressive dynamic modulus of individual constructs increased over time ($p < .01$). No significant differences were observed between METS (pooled average for all regions) and individual construct controls at Day 21 and Day 28 ($p > .19$). (B) GAG content normalized by DNA content (GAG/DNA) of constructs increased over time ($p < .0001$, one-way ANOVA with respect to time). *Represents significant differences in GAG/DNA between METS and individual controls ($p < .002$, Student's *t*-test). Data shown from 2 × 2 METS.

to compare local biochemistry in the bonds to the local biochemistry in the bulk construct. Unpolarized Raman spectra were acquired in backscattering geometry to provide local information on a broad range of matrix constituents (Labram spectrometer, JY-Horiba Scientific, Edison, NJ), equipped with a high-resolution grating (1800 grooves/mm).

The objective of this study was to demonstrate feasibility; therefore, statistical analyses were not performed on mechanical and biochemical properties with respect to location in the METS, which would require a high sample size (n = 4–5 per group unless stated otherwise). A one-way ANOVA and a Student's *t*-test was used to compare properties with respect to time (significance: $p \leq .05$). Data are presented as mean ± standard deviation.

3. Results

Stable connections formed between constructs for all METS samples, such that they could be removed from the basket on Day 14. Fibrous tissue was optically observed at the bond site and cell infiltration was observed through histology (Fig. 3A) Raman spectroscopy revealed peaks corresponding to collagen (880 cm^{-1} and 1655 cm^{-1}), GAGs (1060 cm^{-1}), and other organic matter (e.g., lipids, proteins, etc.; 1454 cm^{-1}; Fig. 3B). A similar response was observed for tissue at the bond site and within the construct, but with lower signal intensity at the bond site due to lower matrix deposition (Fig. 3B – black versus grey lines).

The bonds continued to increase in size and strength over time, with formation of rigid engineered cartilage sheets by Day 21 that could be handled without visible deformation or breaking (2 × 2 METS: final bond width = 2.2 ± 0.3 mm; $p < .05$, bond strength Day 21 versus 28; Fig. 3C and D). Similarly, for 5 × 5 METS, there was a 4-fold increase in the tensile peak force from 0.15 ± 0.16 N on Day 14 to 0.60 ± 0.13 N on Day 28 and 0.53 ± 0.27 N on Day 42 ($p = .04$). Macrochannels that formed remained open throughout culture.

Compressive mechanical properties and biochemical composition of all METS groups and individual constructs increased with time until Day 28 (ANOVA $p < .03$; 2 × 2 METS: Fig. 4). The compressive moduli of all METS groups on Day 28 were on average 5 times greater than initial properties (*t*-test $p < .03$). In 2 × 2 constructs, there was a significant decrease in modulus for both METS and control constructs by Day 42, which was attributed to issues with the culture rather than the METS technique ($p < .05$). Spatial distribution in mechanical and biochemical properties was assessed (Figs. 4–6).

The irregular geometry of the patient-specific basket resulted in a METS sample with three-dimensional contours and topography that matched the cadaveric specimen (Fig. 2D). Histological staining was positive for aggrecan throughout the engineered cartilage surface, suggesting that the patient-specific specimen received sufficient nutrient diffusion for continued tissue production (Fig. 2E).

4. Discussion

This study demonstrated that modular fabrication through self-adhesion is a viable technique for creating large engineered carti-

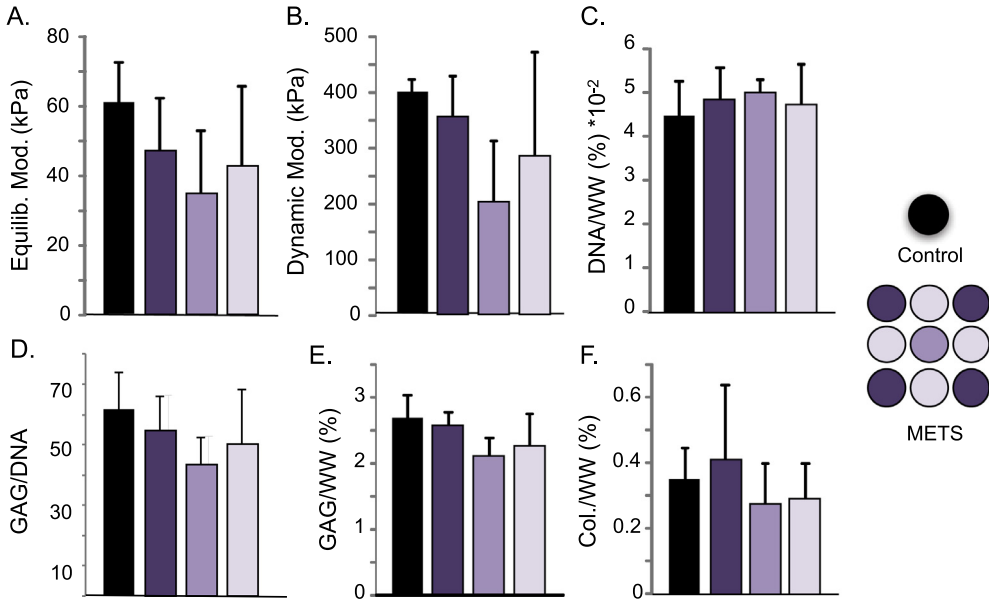

Fig. 5. Dependence on construct location of (A) equilibrium compressive modulus, (B) dynamic modulus, and biochemical properties, including (C) DNA/ww%, (D) GAG/DNA, (E) GAG/ww%, and (F) collagen/ww% of individual controls and 3 × 3 METS (data from 3 × 3 METS, Day 28). No significant differences were observed among controls and METS ($p > .07$, one-way ANOVA).

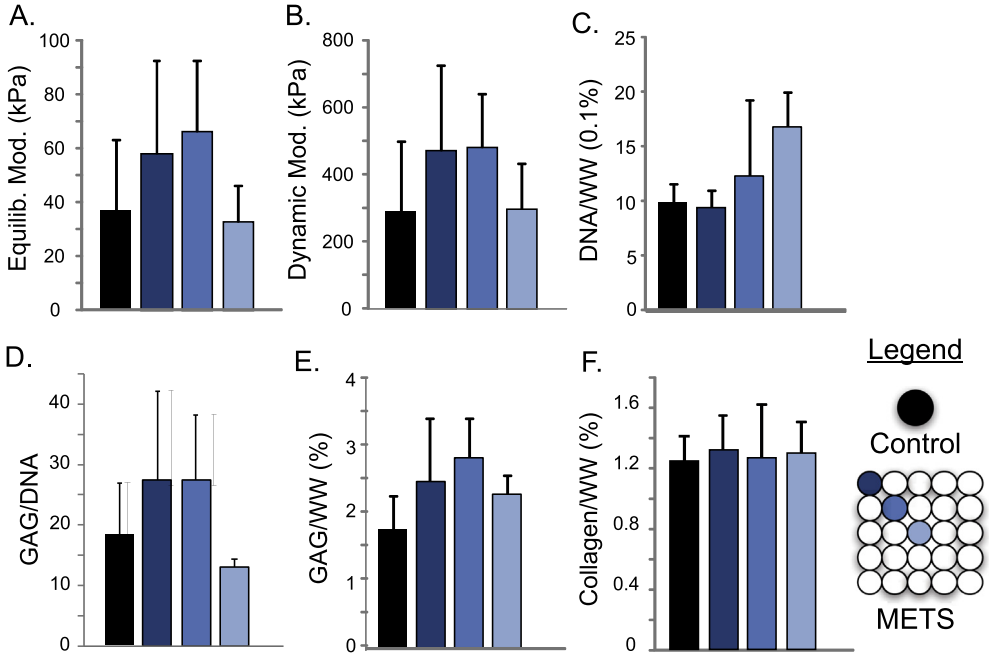

Fig. 6. Dependence on construct location of the (A) equilibrium and (B) dynamic compressive moduli of individual constructs and 5 × 5 METS. (C) DNA/ww%, (D) GAG/DNA, (E) GAG/ww%, and (F) collagen/ww% for individual controls and METS (Day 28).

lage. The METS technique is a method using tight-fit 3D printed porous baskets to encourage construct attachment among individual constructs into larger surfaces and may also act to decrease swelling during *de novo* tissue development from high GAG deposition (Nims et al., 2017). Cells within the bond site continued to deposit extracellular matrix throughout the culture period, increasing failure strength and overall compressive modulus.

Cell infiltration into the bond site was observed histologically, suggesting that cell migration occurred in proximity of neighboring constructs as has been previously seen (Bhumiratana et al., 2014; Mori et al., 2014; Dikina et al., 2015). Raman spectroscopy of the bond site and construct was similar to spectra for human cartilage (Kunstar et al., 2012; Esmonde-White, 2014; Gamsjaeger et al., 2014). Raman peaks for collagen were lower than those for GAG agreeing with biochemical assays and previous work (O'Connell et al., 2013; Cigan et al., 2014; Mesallati et al., 2017). Future work will focus on determining the microstructure, composition, and localized mechanics of the bond.

Biochemical composition and mechanical properties from the outer constructs were comparable to properties measured at the center and to individual constructs. We recognize that a small sample size precludes a claim of improved spatial distribution of

properties. However, we saw no indication of a negative impact with increased total size (Figs. 5 and 6). The creation of METS with large patient specific geometry (>950 mm^2) demonstrated the potential of the technique to be customized for the specific application, eliminating additional steps, material, and time wasted to fit or resize a scaffold to the patient.

Clinically, the METS technique holds good potential as a tissue-engineering analogue to mosaicplasty repair, by which a surgeon grafts smaller circular punches of cartilage into a large defect. However, it not known whether long-term presence of channels are beneficial. Studies using macrochannels showed that channels occlude over time in culture (Bian et al., 2009). Additional work is needed to optimize the size and longevity requirements of channels during METS development.

We recognize the limitations inherent in clinical translation of cell-based approaches that use high cell densities to cultivate engineered tissues. Juvenile bovine cells are the ideal animal source for proof-of-concept studies, but they are not indicative of the behavior from adult human cells. Future work will focus on determining whether METS bonds are stable enough to withstand shear loads in vitro and physiological loading in situ.

The METS approach described in this study builds upon established tissue engineering techniques of developing constructs with GAG composition and compressive mechanical properties towards native cartilage. In conclusion, the METS technique presents a method for creating engineered cartilage surfaces on clinically relevant scales by exploiting the well-known, but underutilized stickiness of *de novo* tissue.

Acknowledgements

This study was supported by the Rose Hills Innovator Award, R01 DE019284, DOD/PRORP OR130191, P30 AR061312-01, a fellowship from Achievement Rewards for College Scientists (ARCS) Foundation Northern California Chapter (Audrey Ford), and undergraduate research fellowships from the Berkeley Stem Cell Center (Aditya Nandy), BeeHive work study program (Aditya Nandy and Anne Zeng), and Student Mentoring and Research Teams (Audrey Ford and Wan Fung Chui). The authors would like to thank Mr. Adam Updegrove for his training with SimVascular software.

Conflict of interest

No competing financial interests exist.

References

Awada, H.A., Wickhama, M.Q., Leddya, H.A., Gimbleb, J.M., Guilak, F., 2004. Chondrogenic differentiation of adipose derived adult stem cells in agarose, alginate, and gelatin scaffolds. Biomaterials 25, 3211–3222.

Benya, P.D., Shaffer, J.D., 1982. Dedifferentiated chondrocytes reexpress the differentiated collagen phenotype when cultured in agarose gels. Cell 30, 215–224.

Bhumiratana, S., Eton, R.E., Oungoulian, S.R., Wan, L.Q., Ateshian, G.A., Vunjak-Novakovic, G., 2014. Large, stratified, and mechanically functional human cartilage grown in vitro by mesenchymal condensation. Proc. Natl. Acad. Sci. USA 111 (19), 6940–6945.

Bian, L., Angione, S.L., Ng, K.W., Lima, E.G., Williams, D.Y., Mao, D.Q., Ateshian, G.A., Hung, C.T., 2009. Influence of decreasing nutrient path length on the development of engineered cartilage. Osteoarthritis Cartilage 17 (5), 677–685.

Bian, L., Fong, J.V., Lima, E.G., Stoker, A.M., Ateshian, G.A., Cook, J.L., Hung, C.T., 2010. Dynamic mechanical loading enhances functional properties of tissue-engineered cartilage using mature canine chondrocytes. Tissue Eng. Part A 16 (5), 1781–1790.

Buckley, C.T., Meyer, E.G., Kelly, D.J., 2012. The influence of construct scale on the composition and functional properties of cartilaginous tissues engineered using bone marrow-derived mesenchymal stem cells. Tissue Eng. Part A 18 (3–4), 382–396.

Chahine, N.O., Albro, M.B., Lima, E.G., Wei, V.I., Dubois, C.R., Hung, C.T., Ateshian, G. A., 2009. Effect of dynamic loading on the transport of solutes into agarose hydrogels. Biophys. J. 97 (4), 968–975.

Cigan, A.D., Nims, R.J., Albro, M.B., Vunjak-Novakovic, G., Hung, C.T., Ateshian, G.A., 2014. Nutrient channels and stirring enhanced the composition and stiffness of large cartilage constructs. J. Biomech. 47 (16), 3847–3854.

Cigan, A.D., Durney, K.M., Nims, R.J., Vunjak-Novakovic, G., Hung, C.T., Ateshian, G. A., 2016. Nutrient channels aid the growth of articular surface-sized engineered cartilage constructs. Tissue Eng. Part A 22, 1063–1074.

Cohen, Z.A., McCarthy, D.M., Kwak, S.D., Legrand, P., Fogarasi, F., Ciaccio, E.J., Ateshian, G.A., 1999. Knee cartilage topography, thickness, and contact areas from MRI: in-vitro calibration and in-vivo measurements. Osteoarthritis Cartilage 7 (1), 95–109.

Dikina, A.D., Strobel, H.A., Lai, B.P., Rolle, M.W., Alsberg, E., 2015. Engineered cartilaginous tubes for tracheal tissue replacement via self-assembly and fusion of human mesenchymal stem cell constructs. Biomaterials 52, 452–462.

DuRaine, G.D., Brown, W.E., Hu, J.C., Athanasiou, K.A., 2015. Emergence of scaffold-free approaches for tissue engineering musculoskeletal cartilages. Ann. Biomed. Eng. 43 (3), 543–554.

Eniwumide, J.O., Lee, D.A., Bader, D.L., 2009. The development of a bioreactor to perfuse radially-confined hydrogel constructs: design and characterization of mass transport properties. Biorheology 46 (5), 417–437.

Erickson, I.E., Kestle, S.R., Zellars, K.H., Dodge, G.R., Burdick, J.A., Mauck, R.L., 2012. Improved cartilage repair via in vitro pre-maturation of MSC-seeded hyaluronic acid hydrogels. Biomed. Mater. 7 (2), 024110.

Esmonde-White, K., 2014. Raman spectroscopy of soft musculoskeletal tissues. Appl. Spectrosc. 68 (11), 1203–1218.

Farrell, M.J., Comeau, E.S., Mauck, R.L., 2012. Mesenchymal stem cells produce functional cartilage matrix in three-dimensional culture in regions of optimal nutrient supply. Eur. Cell Mater. 23, 425–440.

Gadjanski, I., Vunjak-Novakovic, G., 2015. Challenges in engineering osteochondral tissue grafts with hierarchical structures. Expert Opin. Biol. Ther. 15 (11), 1583–1599.

Gamsjaeger, S., Klaushofer, K., Paschalis, E.P., 2014. Raman analysis of proteoglycans simultaneously in bone and cartilage. J. Raman Spectrosc. 45 (9), 794–800.

Kelly, T.A., Ng, K.W., Wang, C.C., Ateshian, G.A., Hung, C.T., 2006. Spatial and temporal development of chondrocyte-seeded agarose constructs in free-swelling and dynamically loaded cultures. J. Biomech. 39 (8), 1489–1497.

Khoshgoftar, M., Wilson, W., Ito, K., van Donkelaar, C.C., 2013. The effect of tissue-engineered cartilage biomechanical and biochemical properties on its post-implantation mechanical behavior. Biomech. Model Mechanobiol. 12 (1), 43–54.

Kock, L.M., Malda, J., Dhert, W.J., Ito, K., Gawlitta, D., 2014. Flow-perfusion interferes with chondrogenic and hypertrophic matrix production by mesenchymal stem cells. J. Biomech. 47 (9), 2122–2129.

Kunstar, A., Leijten, J., van Leuveren, S., Hilderink, J., Otto, C., van Blitterswijk, C.A., Karperien, M., van Apeldoorn, A.A., 2012. Recognizing different tissues in human fetal femur cartilage by label-free Raman microspectroscopy. J. Biomed. Opt. 17 (11), 116012.

Lima, E.G., Durney, K.M., Sirsi, S.R., Nover, A.B., Ateshian, G.A., Borden, M.A., Hung, C. T., 2012. Microbubbles as biocompatible porogens for hydrogel scaffolds. Acta Biomater. 8 (12), 4334–4341.

Makris, E.A., Gomoll, A.H., Malizos, K.N., Hu, J.C., Athanasiou, K.A., 2015. Repair and tissue engineering techniques for articular cartilage. Nat. Rev. Rheumatol. 11 (1), 21–34.

Mauck, R.L., Soltz, M.A., Wang, C.C., Wong, D.D., Chao, P.H., Valhmu, W.B., Hung, C.T., Ateshian, G.A., 2000. Functional tissue engineering of articular cartilage through dynamic loading of chondrocyte-seeded agarose gels. J. Biomech. Eng. 122 (3), 252–260.

Mesallati, T., Buckley, C.T., Kelly, D.J., 2017. Engineering cartilaginous grafts using chondrocyte-laden hydrogels supported by a super fi cial layer of stem cells. J. Tissue Eng. Regener. Med. 11, 1343–1353.

Mori, Y., Kanazawa, S., Asawa, Y., Sakamoto, T., Inaki, R., Okubo, K., Nagata, S., Komura, M., Takato, T., Hoshi, K., 2014. Regenerative cartilage made by fusion of cartilage elements derived from chondrocyte sheets prepared in temperature-responsive culture dishes. J. Hard Tissue Biol. 23 (1), 101–110.

Natoli, R.M., Revell, C.M., Athanasiou, K.A., 2009. Chondroitinase ABC treatment results in greater tensile properties of self-assembled tissue-engineered articular cartilage. Tissue Eng. Part A 15 (10), 3119–3128.

Nichol, J.W., Khademhosseini, A., 2009. Modular tissue engineering: engineering biological tissues from the bottom up. Soft Matter 5 (7), 1312–1319.

Nims, R.J., Cigan, A.D., Albro, M.B., Hung, C.T., Ateshian, G.A., 2014. Synthesis rates and binding kinetics of matrix products in engineered cartilage constructs using chondrocyte-seeded agarose gels. J. Biomech. 47 (9), 2165–2172.

Nims, R.J., Cigan, A.D., Albro, M.B., Vunjak-Novakovic, G., Hung, C.T., Ateshian, G.A., 2015. Matrix production in large engineered cartilage constructs is enhanced by nutrient channels and excess media supply. Tissue Eng. Part C Method 21 (7), 747–757.

Nims, R.J., Cigan, A.D., Durney, K.M., Jones, B.K., O'Neill, J.D., Law, W.-S.A., Ateshian, G.A., 2017. Constrained cage culture improves engineered cartilage functional properties by enhancing collagen network stability. Tissue Eng. Part A.

Nover, A.B., Jones, B.K., Yu, W.T., Donovan, D.S., Podolnick, J.D., Cook, J.L., Ateshian, G. A., Hung, C.T., 2016. A puzzle assembly strategy for fabrication of large engineered cartilage tissue constructs. J. Biomech. 49 (5), 668–677.

O'Connell, G.D., Leach, J.K., Klineberg, E.O., 2015a. Tissue engineering a biological repair strategy for lumbar disc herniation. Biores. Open Access 4 (1), 431–445.

O'Connell, G.D., Lima, E.G., Bian, L., Chahine, N.O., Albro, M.B., Cook, J.L., Ateshian, G. A., Hung, C.T., 2013. Toward engineering a biological replacement. J. Knee Surg. 46 (11), 1784–1791.

O'Connell, G.D., Nims, R.J., Green, J., Cigan, A.D., Ateshian, G.A., Hung, C.T., 2014. Time and dose-dependent effects of chondroitinase ABC on growth of engineered cartilage. Eur. Cell Mater. 27, 312–320.

O'Connell, G.D., Tan, A.R., Palmer, G.D., Cui, V.H., Bulinski, J.C., Ateshian, G.A., Hung, C.T., 2015b. Cell migration behavior of human chondrocytes for guiding three-dimensional engineered cartilage growth. Tissue Eng. Regen. Med. in press, PMID: 25627968.

Wilson, N., Wang, K., Dutton, R.W., Taylor, C., 2001. A software frameowrk for creating patient specific geometric models from medical imaging data for simulation based medical planning of vascular surgery. Springer, pp. 449–456.